International Journal of Scientific Research in Engineering and Management (IJSREM)
Volume: 09 Issue: 11 | Nov - 2025 SJIF Rating: 8.586 ISSN: 2582-3930

Artificial Intelligence–Based Structural Health Monitoring of Aging Reinforced Concrete Bridges Using Sap2000 Simulation and Vibration Data Analysis

Chetan Milapchand Jogad[2], Satish Sahebrao Manal[2]

[2]MTech Student, Department of Civil Engineering, Chh. Shahu College of Engineering, Chhatrapati Sambhajinagar

[2]Assistant Professor, CSMSS, Chh. Shahu College of Engineering, Chhatrapati Sambhajinagar

Abstract

The study presents a hybrid Artificial Intelligence–based Structural Health Monitoring (SHM) framework for aging reinforced concrete highway bridges, integrating SAP2000 finite element simulations with vibration data analysis. Two multi-span bridges—an older span and a newly strengthened span—were instrumented and tested under controlled vehicular loading using 35-ton and 45-ton trucks at varying speeds between 40–80 km/h. Field measurements of acceleration and deflection were obtained through high-frequency sensors and Fast Fourier Transform (FFT) analysis and compared with numerical simulations. Results indicated that bridge response is highly sensitive to vehicle speed and load, with Dynamic Amplification Factors (DAF) ranging from approximately 1.00–2.35 for the old bridge and 1.00–1.89 for the new bridge. The integration of experimental data with a Convolutional Neural Network (CNN) model significantly improved predictive accuracy, achieving R^2 values above 0.80 when benchmarked against FEM outputs and approximately 0.99 when compared with field data. The hybrid CNN–DAF framework effectively enhances the reliability of structural response prediction, maintaining modal consistency while addressing the limitations of traditional FEM analysis. This approach provides a robust, data-driven solution for continuous bridge health monitoring, enabling proactive maintenance, extended service life, and improved safety of critical transportation infrastructure.

Keywords: Structural Health Monitoring, Artificial Intelligence, SAP2000, Convolutional Neural Network, Dynamic Amplification Factor

1. INTRODUCTION

Bridges are essential components of global transportation infrastructure, facilitating the movement of people, goods, and services that drive economic growth and societal progress. However, a significant number of reinforced concrete (RC) bridges have surpassed their original design life, leading to deterioration caused by aging, corrosion, environmental exposure, fatigue, and increased vehicular loads. These factors threaten the structural integrity and serviceability of bridges, making regular performance assessment vital for public safety. Traditional inspection methods, such as visual surveys and manual testing, are often subjective, time-consuming, and incapable of detecting internal or progressive damage between inspection intervals. This limitation highlights the urgent need for intelligent and automated systems capable of continuous, real-time monitoring. Structural Health Monitoring (SHM) has emerged as an advanced solution that employs sensors, data acquisition units, and analytical tools to track a bridge's performance and detect damage at an early stage. However, traditional SHM systems often struggle to process the massive and complex datasets produced by modern sensing networks. To overcome these challenges, Artificial Intelligence (AI) has become a transformative tool in SHM, utilizing machine learning and deep learning algorithms for automated data analysis, pattern recognition, and predictive maintenance.

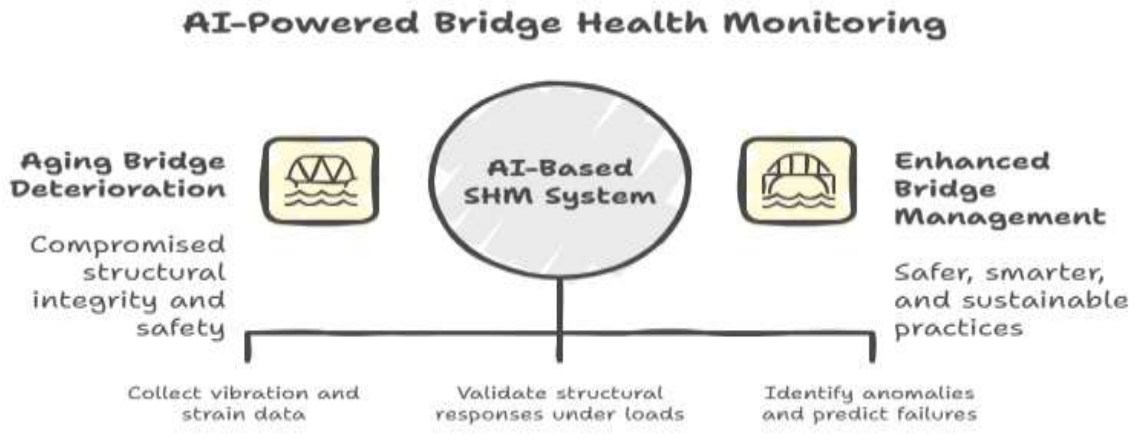

Fig 1: AI- Powered Bridge Health Monitoring

AI-based SHM systems employ models such as Artificial Neural Networks (ANN), Support Vector Machines (SVM), and Convolutional Neural Networks (CNN) to analyze vibration and strain data, identify anomalies, and predict potential failures. When integrated with Finite Element Analysis (FEA) tools like SAP2000, these systems can develop a "digital twin" that mirrors the physical condition of the bridge in real time. Combining AI with vibration-based methods, including Fast Fourier Transform (FFT) and time–frequency analysis, enhances diagnostic precision. This study aims to develop an AI-driven SHM framework using SAP2000 simulations and vibration data to enable continuous, automated, and accurate assessment of aging RC bridges for safer and more sustainable infrastructure management.

2. RELATED WORK

Limin Sun et al. (2020) reviewed the role of Big Data (BD) and Artificial Intelligence (AI) in enhancing Structural Health Monitoring (SHM) of long-span bridges. The study emphasized that traditional SHM methods struggle to interpret massive and complex datasets effectively. BD techniques were categorized into computing frameworks for managing large-scale data and analytical methods for extracting structural insights. Deep learning, representing AI applications, was highlighted for its strength in processing unstructured data such as images and time-series signals to detect structural damage. The authors concluded that integrating BD and AI enables intelligent, data-driven SHM systems, while outlining existing challenges, computational limits, and future research opportunities. **Raffaele Zinno et al. (2022)** examined the transformative role of Artificial Intelligence (AI), the Internet of Things (IoT), and big data analytics in advancing Structural Health Monitoring (SHM) systems within the framework of smart cities. The study emphasized that AI enhances the flexibility, robustness, and analytical capacity of SHM for critical infrastructures such as bridges, which are highly vulnerable to environmental and operational stresses. It reviewed AI-driven, data-centric SHM frameworks applied throughout the bridge life cycle—from construction to maintenance—highlighting their integration with Intelligent Transportation Systems (ITS). The paper concluded by identifying key advantages, current limitations, and promising research directions for developing next-generation AI-assisted SHM solutions for sustainable bridge management. https://doi.org/10.1109/ACCESS.2022.3199443 **Mateo Clement et al. (2024)** proposed an advanced Structural Health Monitoring (SHM) framework that integrates Artificial Intelligence (AI) and Internet of Things (IoT) technologies to address the growing deterioration of aging steel girder bridges. The study emphasized that traditional inspection methods are inadequate for detecting early-stage defects caused by fatigue, corrosion, and dynamic loads. The proposed system employs a distributed IoT sensor network—comprising accelerometers, strain gauges, and ultrasonic transducers—to continuously collect high-frequency structural data. Deep learning-based predictive analytics are used to identify anomalies, predict failures, and trigger preventive alerts. A case study demonstrated improved accuracy and maintenance efficiency, proving AI–IoT integration as a scalable, real-time, and cost-effective approach for ensuring bridge safety and extending service life. https://www.researchgate.net/profile/Mateo-Clement/publication/390416666_Advanced_Structural_Health_Monitoring_for_Aging_Steel_Girder_Bridges_Using_AI_and_IoT_Sensors/links/67ecf4ce95231d5ba5abac42/Advanced-Structural-Health-Monitoring-for-Aging-Steel-Girder-Bridges-Using-AI-and-IoT-Sensors.pdf

Sharan Kumar et al. (2025) presented a machine learning-based Structural Health Monitoring (SHM) approach for railway truss bridges aimed at overcoming the limitations of traditional inspection methods that are often slow and error-prone. The proposed method utilizes vibration responses recorded under moving train loads and applies signal processing techniques such as wavelet transforms, Fourier analysis, and spectrograms to extract damage-related features. To address challenges in field data collection, the study employs a numerical bridge model with simulated train loads to generate acceleration data for multiple damage scenarios. Various machine learning algorithms, including decision trees and residual neural networks, were trained on this dataset, successfully identifying damaged bridge members. The study highlights machine learning's potential to improve accuracy and efficiency in bridge SHM while emphasizing the continued importance of expert interpretation for final assessment. https://doi.org/10.1007/s44290-025-00199-8 **Raffaele Zinno et al. (2022)** examined the integration of advanced technologies such as Artificial Intelligence (AI), the Internet of Things (IoT), drone technology, and 3D printing in enhancing Structural Health Monitoring (SHM) systems for smart cities. The study highlighted that growing urban populations and infrastructure demands necessitate intelligent, technology-driven solutions. Bridges, being vital urban assets, can benefit greatly from AI- and IoT-enabled SHM frameworks that enable real-time monitoring, predictive maintenance, and extended structural life. The paper presented conceptual models, discussed benefits and challenges, and identified future research opportunities for developing smart, efficient, and sustainable bridge management systems. https://doi.org/10.3390/app13010097 **Vijay Prakash et al. (2025)** presented a comprehensive review on the application of Artificial Intelligence (AI) in the Structural Health Monitoring (SHM) of concrete bridges, emphasizing the growing demand for efficient and accurate inspection methods. The study highlighted that conventional manual inspections are time-consuming, subjective, and prone to human error, whereas AI-based approaches, particularly Machine Learning and Deep Learning, provide automated and precise damage detection. Special focus was given to crack detection and assessment accuracy in various bridge types. The authors concluded that integrating multimodal AI techniques enhances monitoring reliability, spatial resolution, and long-term maintenance efficiency of concrete bridge structures. https://doi.org/10.3390/app15094855

2.1 Research gap

Although considerable progress has been made in applying Artificial Intelligence, Internet of Things (IoT), and Big Data analytics to Structural Health Monitoring (SHM), several research gaps persist. Existing studies predominantly focus on steel or truss bridges, leaving limited exploration of aging reinforced concrete (RC) bridges that exhibit complex deterioration mechanisms. Most frameworks rely heavily on theoretical or simulation-based models without sufficient validation through real-time vibration data or integration with advanced finite element tools such as SAP2000. Furthermore, challenges related to sensor noise, environmental variability, data fusion, and adaptive learning models remain unresolved. There is a need for a robust hybrid AI–FEA approach that combines SAP2000 simulation with vibration-based data analysis for continuous, accurate, and intelligent health monitoring of aging RC bridges.

3. RESEARCH METHODOLOGY

3.1 Overview and Study Design

This study presents a hybrid Structural Health Monitoring (SHM) framework integrating physics-based modeling, field sensing, and deep learning for accurate bridge damage detection under real-world conditions. Field experiments provide vibration and strain data, while a SAP2000 finite element (FE) "digital twin" simulates bridge responses and establishes baseline modal properties. Non-stationary signals are processed using time–frequency analysis to capture modal drift and damping variations. A grouped Convolutional Neural Network (CNN-Group) processes multi-view inputs—raw data, time–frequency maps, and FE priors—to classify structural states. The system operates in a closed feedback loop, enabling continuous monitoring, calibration, and maintenance decision-making for enhanced safety and life-cycle management.

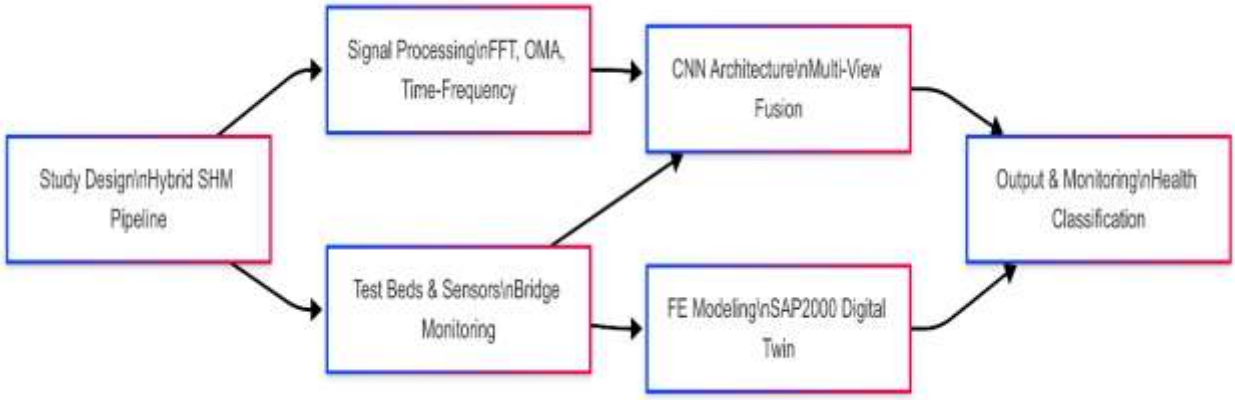

Fig. 2. Research Method Flow

3.2 Test Beds, Sensors, and Data Acquisition

Field data were collected from two multi-span highway bridges over the Panchganga River—one aging and one prestressed concrete bridge. Around ten sensor locations per bridge recorded vibrations and strains using tri-axial accelerometers and strain gauges. Controlled vehicle runs and ambient traffic were used to capture realistic dynamic responses. The resulting dataset combines labeled experiments and real-world variability, ensuring model robustness under diverse traffic and environmental conditions.

3.3 Finite Element Modeling and Simulation

A detailed SAP2000 model was developed using shell and frame elements for deck, girders, abutments, and piers. Vehicle loads were simulated as moving axle forces to replicate experimental conditions. Modal properties—frequencies, shapes, and damping—were extracted and calibrated with field data. Damage conditions were modeled by reducing localized stiffness to generate synthetic examples. This FE-based digital twin provided physics-grounded priors and reference indicators for training and validation.

3.4 Signal Processing

Raw acceleration and strain signals were detrended, filtered, synchronized, and normalized. FFT and adaptive time–frequency techniques (Hilbert–Huang transforms) captured modal changes and transient behaviors. Operational Modal Analysis (OMA) estimated frequency and damping variations under ambient conditions. The resulting spectra, time–frequency maps, and OMA features formed the multi-view evidence for health classification.

3.5 CNN-Group Architecture, Training, and Validation

The CNN-Group architecture processed three synchronized inputs—raw signals, time–frequency images, and FE-derived features—through specialized subnetworks. Their embeddings were fused to produce calibrated health probabilities. Training incorporated

regularization, resampling, and cross-validation across bridges. Model confidence was refined through post-hoc temperature scaling, and predictions were combined with modal drift indicators to trigger precise and reliable maintenance alarms.

4. RESULTS AND DISCUSSION

The results show that higher vehicle speed and load significantly increase bridge displacement and acceleration. Dynamic Amplification Factors rise with velocity, with the old bridge showing greater response. Field–model agreement confirms SAP2000 model accuracy for serviceability assessment and retrofit planning.

4.1 Different mode shapes with Modal frequency and Modal periods

Table 1. Different mode shapes with Modal frequency and Modal periods

Output Case	Step Type	Step Num	Period	Frequency	Circ Freq	Eigen value	Maximum deflection value	Position of maximum deflection
Text	Text	Unit less	Sec	Cycle/sec	Rad /sec	rad^2/sec^2	mm	m
modal	Mode	1	2.108261	0.47432	2.9803	8.882	7.55	10.90
modal	Mode	2	1.612884	0.62001	3.8956	15.176	5.90	10.50
modal	Mode	3	1.549475	0.64538	4.055	16.443	4.35	10.22
modal	Mode	4	1.089546	0.91781	5.7668	33.256	3.12	0.5.36
modal	Mode	5	0.960229	1.0414	6.5434	42.816	1.76	18.00
modal	Mode	6	0.889335	1.1244	7.065	49.915	2.34	3.90
modal	Mode	7	0.773035	1.2936	8.1279	66.063	0.55	2.88
modal	Mode	8	0.709512	1.4094	8.8556	78.422	1.23	5.30
modal	Mode	9	0.637828	1.5678	9.8509	97.04	2.40	6.25
modal	Mode	10	0.614158	1.6282	10.231	104.66	1.00	7.00
modal	Mode	11	0.58923	1.6971	10.663	113.71	0.55	6.20
modal	Mode	12	0.507527	1.9703	12.38	153.26	0.72	6.40

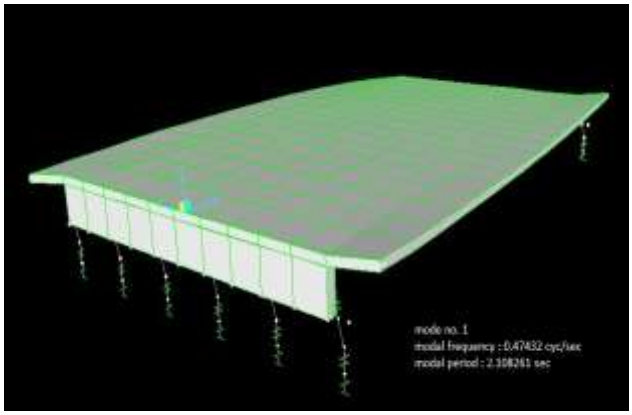

Mode No.1

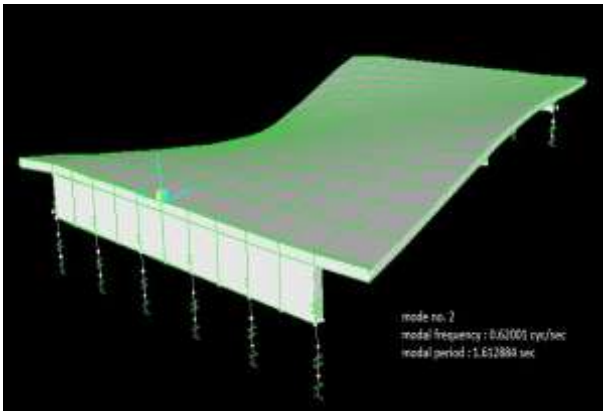

Mode No.2

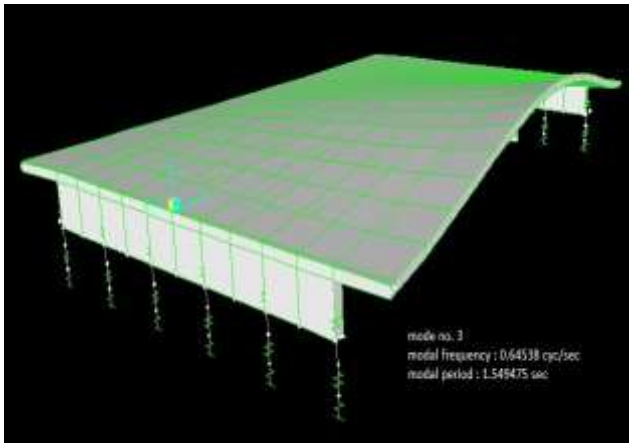

Mode No.3

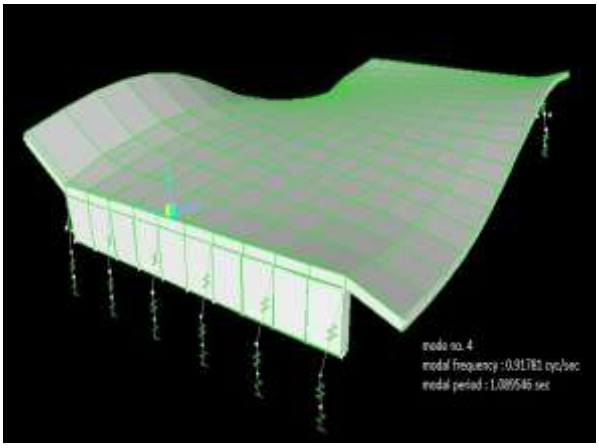

Mode No.4

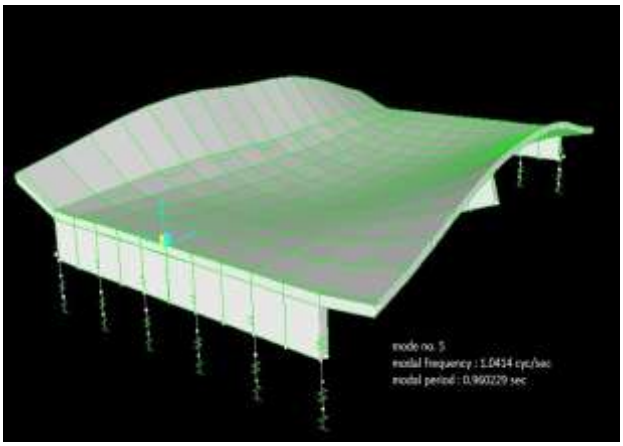

Mode No.5

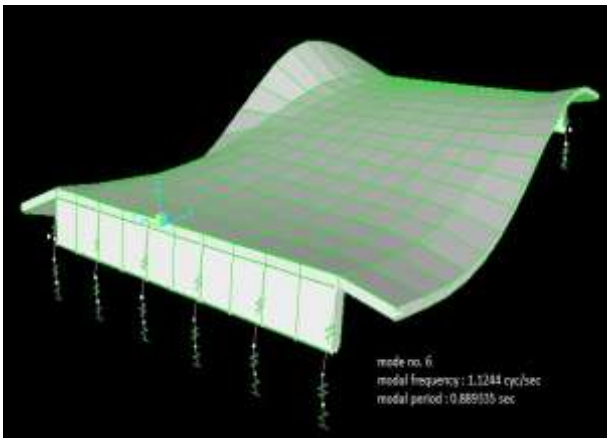

Mode No.6

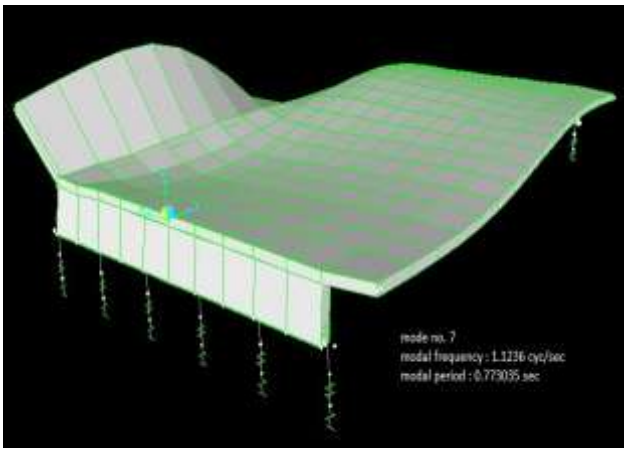

Mode No.7

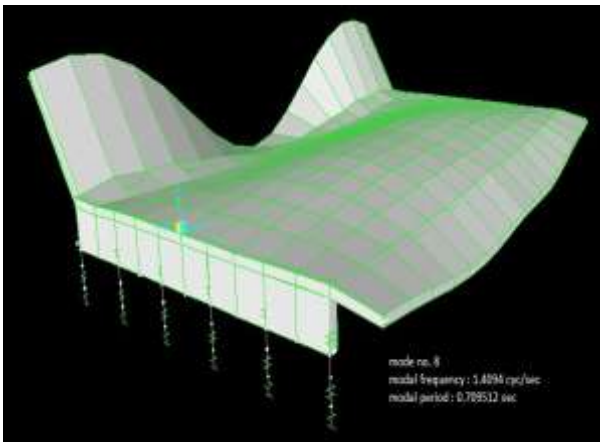

Mode No.8

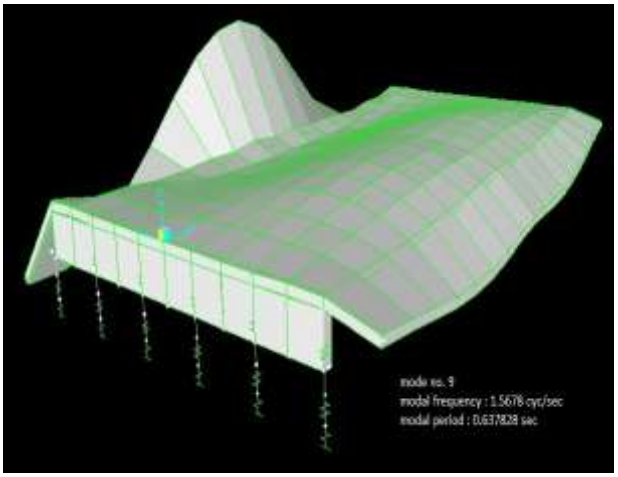

Mode No.9

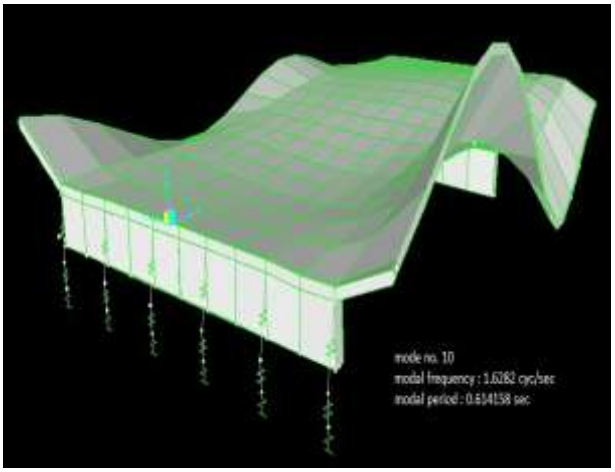

Mode No.10

A result shows that, the maximum modal frequency occurs at mode no. 12 with value 1.9703 cycle/sec. & maximum deflection occurs at first mode with 7.55 mm at 10.90 m distance from zero end. Maximum modal period is observed at mode no. 1 with value 2.10 seconds.

4.1 45-ton weight vehicle with Speed 40 km/h (11.11 m/s)

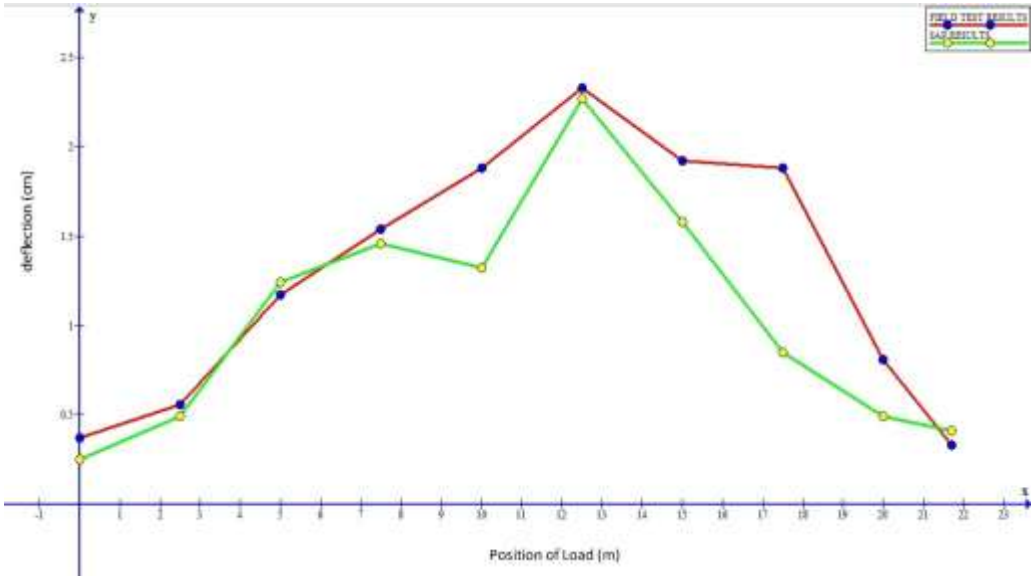

Fig 3. Deflection vs. Position of load along span of bridge (X) for 40 km/h speed

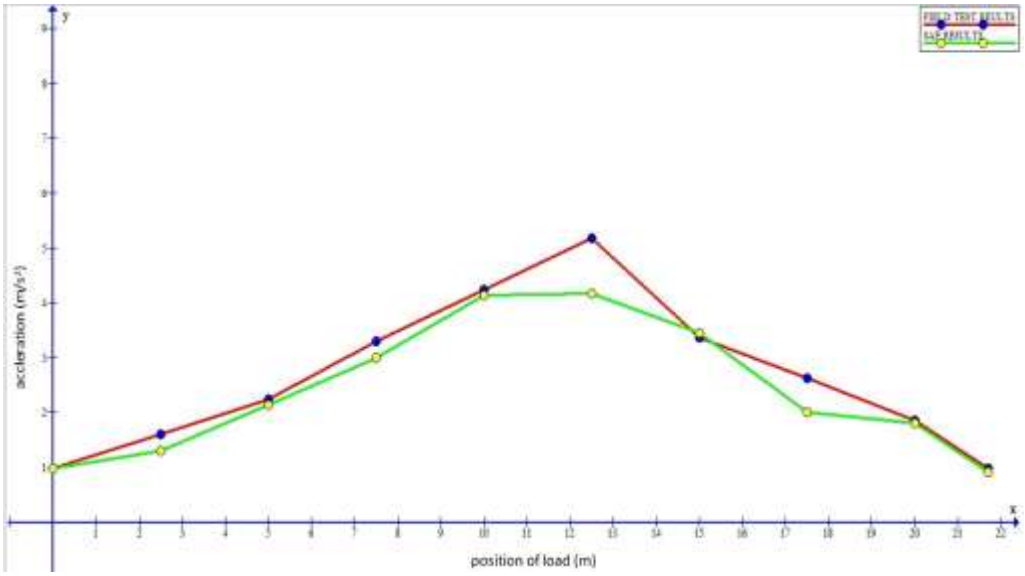

Fig 4: Acceleration vs. Position of load along span of bridge (X) for 40 km/h speed

The results for a 45-ton vehicle traveling at 40 km/h (11.11 m/s) indicate that the maximum displacement of 2.33 cm and maximum acceleration of 5.17 m/s² occur at 12.5 m along the bridge span. Field measurements using an accelerometer closely match SAP analytical predictions, with minor differences in both displacement and acceleration. Displacement generally increases from the start, peaks near mid-span, and then decreases, while acceleration follows a similar trend with slight variations. The data demonstrate that the bridge experiences its highest dynamic response near mid-span under moving load, validating the SAP model's accuracy for predicting structural behavior under heavy vehicular traffic.

4.2 Results for 45-ton weight vehicle with Speed 50 km/h (13.88 m/s)

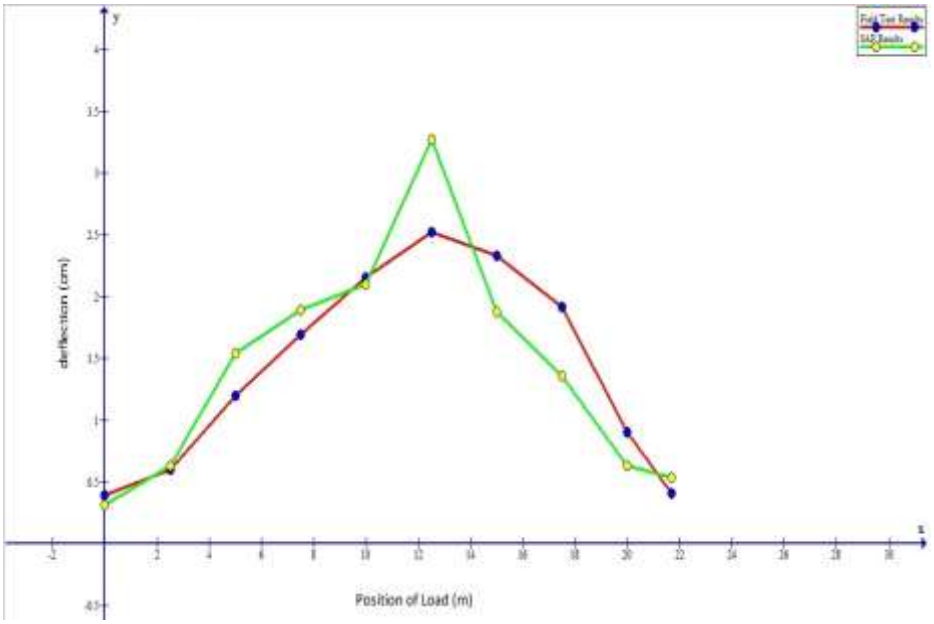

Fig 5: Deflection vs. Position of load along span of bridge for 50 km/h speed

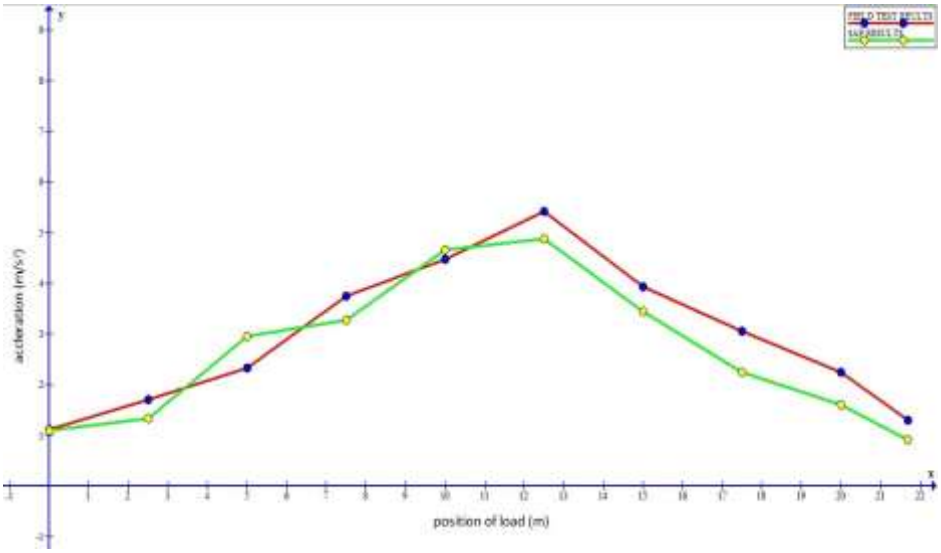

Fig 6: Acceleration vs. Position of load along span of bridge (X) for 50 km/h speed

For a 45-ton vehicle traveling at 50 km/h (13.88 m/s), the bridge experiences a maximum displacement of 2.52 cm and a maximum acceleration of 5.42 m/s², both occurring at 12.5 m from the zero end. Compared to the 40 km/h case, both displacement and acceleration increase slightly due to the higher vehicle speed, reflecting the speed-dependent dynamic amplification of the bridge response. The displacement generally rises toward mid-span and then decreases, while acceleration follows a similar trend. Figures 5 and 6 illustrate the variation of deflection and acceleration along the bridge span, confirming the location of peak dynamic effects and validating the structural response under increased moving load velocity.

4.3 45-ton weight vehicle with Speed 60 km/h (16.67 m/s)

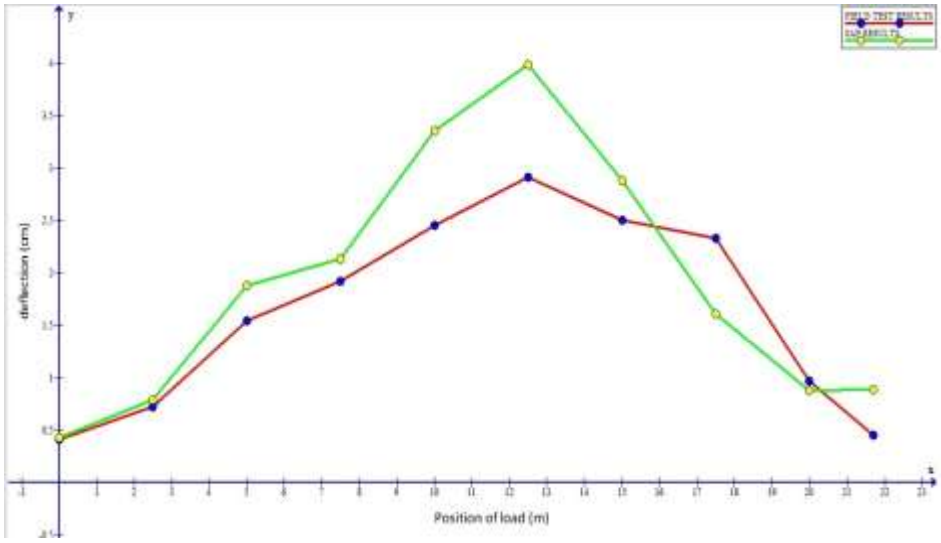

Fig 7: Deflection vs. Position of load along span of bridge (X) for 60 km/h speed

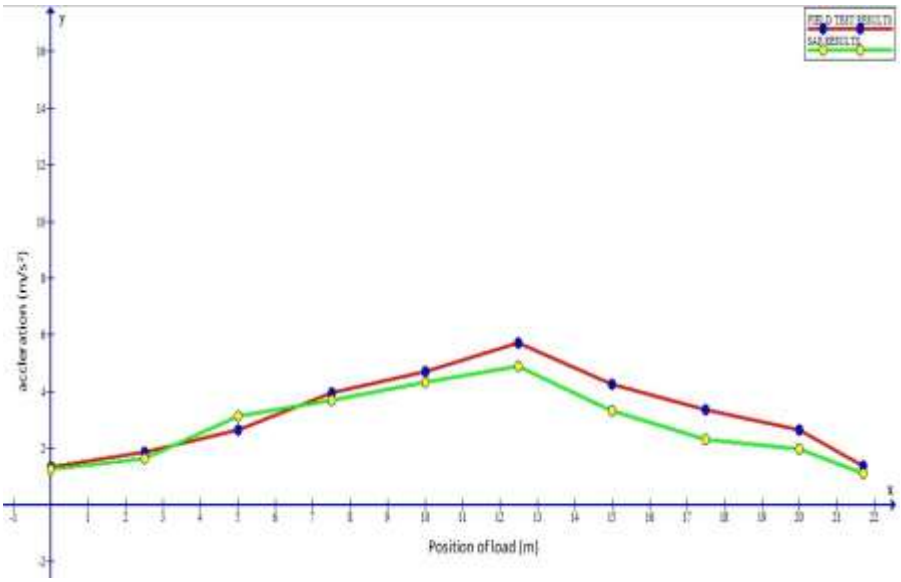

Fig 8: Acceleration vs. Position of load along span of bridge (X) for 60 km/h speed

For a 45-ton vehicle traveling at 60 km/h (16.67 m/s), the bridge experiences a maximum displacement of 2.91 cm and a maximum acceleration of 5.71 m/s² at 12.5 m from the zero end. Compared to lower speeds, both displacement and acceleration increase, highlighting the speed-dependent amplification of dynamic responses. Displacement generally rises toward mid-span before decreasing, while acceleration follows a similar pattern with slight variations. Field test results using an accelerometer show reasonable agreement with SAP analytical predictions, with minor differences attributed to modeling assumptions and real-world conditions. Figures 7 and 8 depict the variation of deflection and acceleration along the bridge span, confirming the location of peak effects under higher-speed loads.

4.4 45-ton weight vehicle with Speed 70 km/h (19.44 m/s)

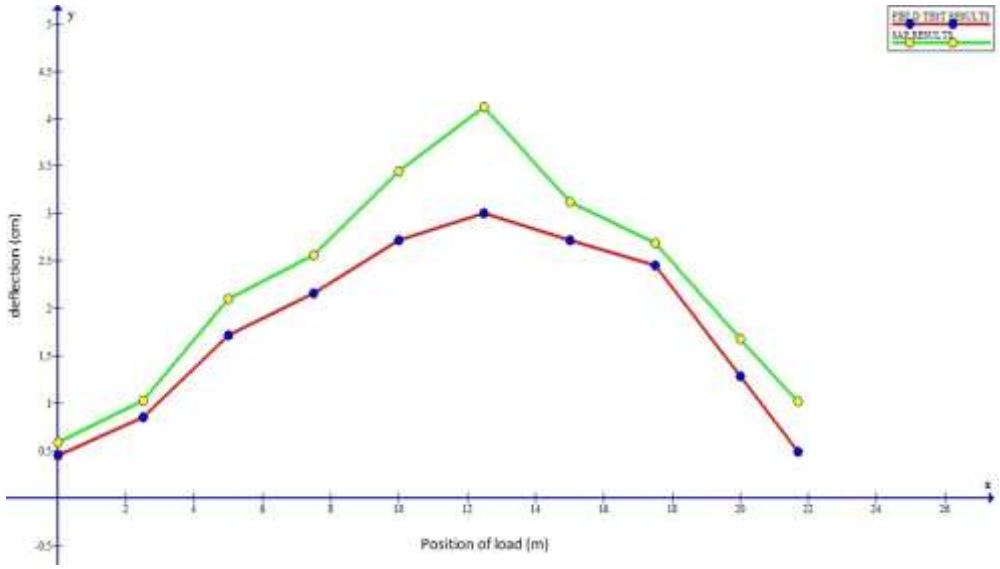

Fig 9: Deflection vs. Position of load along span of bridge for 70 km/h speed

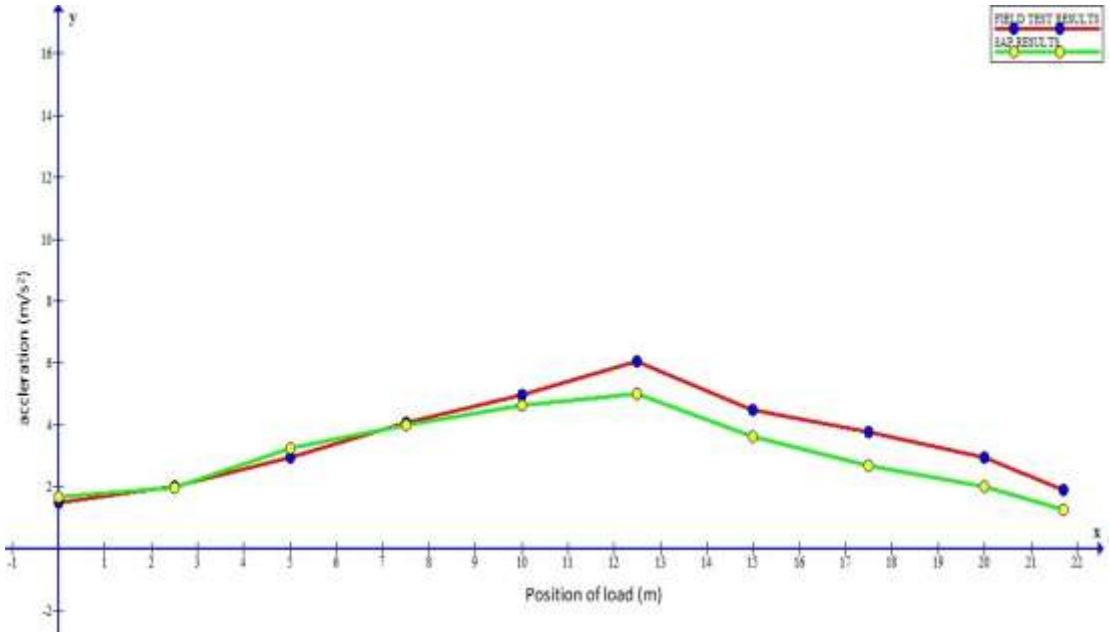

Fig 10: Acceleration vs. Position of load along span of bridge for 70 km/h speed

For a 45-ton vehicle traveling at 70 km/h (19.44 m/s), the bridge experiences a maximum displacement of 3.00 cm and a maximum acceleration of 6.05 m/s², both occurring at 12.5 m from the zero end. Compared to lower speeds, both displacement and acceleration increase, demonstrating the significant effect of higher vehicle speed on dynamic response. Displacement rises toward mid-span and then decreases, while acceleration follows a similar trend with slight variations. Field test results closely align with SAP analytical predictions, with minor differences due to modeling assumptions and real-world conditions. Figures 9 and 10 illustrate the variation of deflection and acceleration along the bridge span under high-speed loading.

4.5 Results for 45-ton weight vehicle with Speed 80 km/h (22.22 m/s)

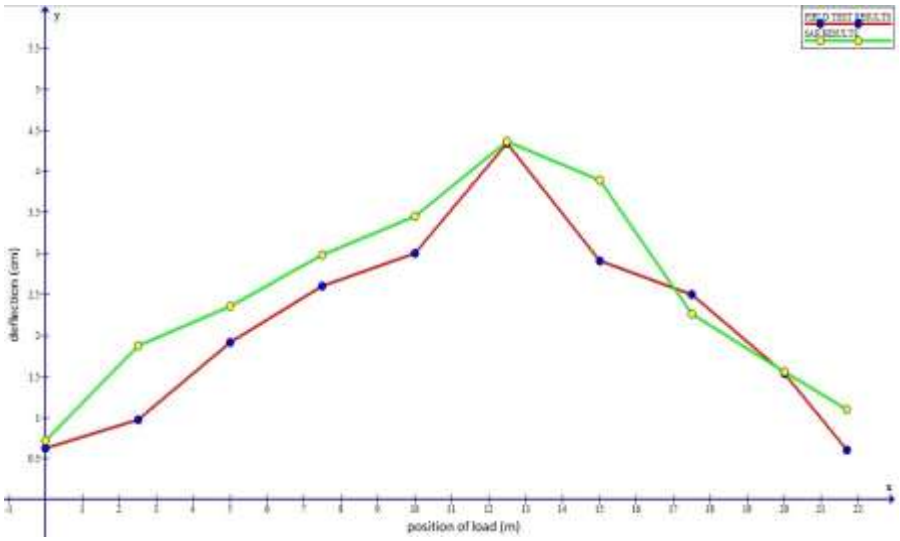

Fig 11: Deflection vs. Position of load along span of bridge (X) for 80 km/h speed

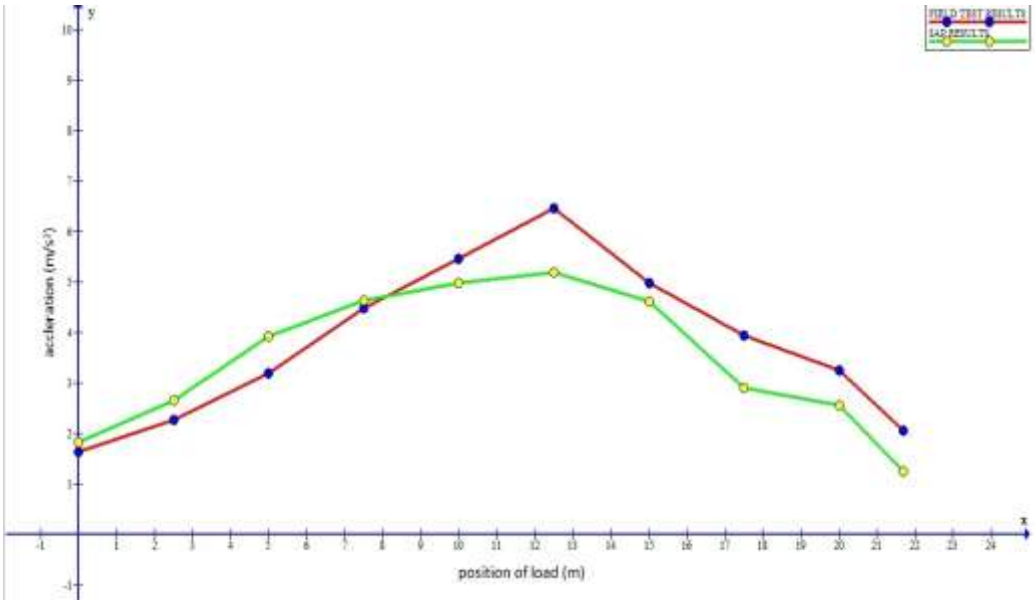

Fig 12: Acceleration vs. Position of load along span of bridge (X) for 80 km/h speed

For a 45-ton vehicle traveling at 80 km/h (22.22 m/s), the bridge shows a maximum displacement of 4.34 cm and a maximum acceleration of 6.45 m/s², both occurring at 12.5 m from the zero end. Compared to lower speeds, the displacement and acceleration increase significantly, indicating pronounced dynamic amplification with higher vehicle velocity. Displacement rises toward mid-span before decreasing, while acceleration follows a similar pattern with slight variations along the span. Field test results using an accelerometer align closely with SAP analytical predictions, with minor deviations due to real-world conditions and modeling assumptions. Figures 11 and 12 depict the deflection and acceleration profiles along the bridge span under the 80 km/h moving load.

4.6 Effect on Deflection & acceleration

Table 2: Effect of 45-Ton Vehicle on Bridge Deflection and Acceleration

Sr. no.	Span	Percentage increase in deflection of deck with increase in weight	Percentage increase in acceleration of deck with increase in weight
		45 ton	45 ton
1	0.0	21.15	19.85
2	2.5	14.12	14.07
3	5.0	13.61	7.77
4	7.5	6.12	10.07

5	10	3.09	5.61
6	12.5	8.23	6.61
7	15.0	6.99	17.22
8	17.5	7.30	18.32
9	20.0	20.31	9.80
10	21.7	35.56	20.47
AVARAGE INCREMENT		13.65	12.98

The table presents the percentage increase in deck deflection and acceleration under a 45-ton vehicle. Maximum deflection increase occurs at 21.7 m (35.56%), while the highest acceleration increase is also at 21.7 m (20.47%). Other spans show moderate variations, with deflection increases ranging from 3.09% to 21.15% and acceleration increases from 5.61% to 19.85%. The average increments across the span are 13.65% for deflection and 12.98% for acceleration. This indicates that heavier vehicular loads significantly amplify both displacement and dynamic response, particularly near supports and at mid-to-end spans, highlighting the importance of accounting for moving load effects in bridge design and assessment.

4.7 Dynamic Amplification Factors for various velocities

Table 3: Dynamic Amplification Factor at Different Vehicle Speeds

Span (m)	40 km/h	50 km/h	60 km/h	70 km/h	80 km/h
0.0	1.12	1.18	1.24	1.36	1.89
2.5	1.03	1.11	1.33	1.57	1.78
5.0	1.03	1.06	1.36	1.52	1.65
7.5	1.01	1.11	1.26	1.42	1.71
10.0	1.02	1.17	1.33	1.47	1.63
12.5	1.01	1.09	1.26	1.30	1.86
15.0	1.06	1.28	1.33	1.50	1.84
17.5	1.09	1.11	1.35	1.42	1.45
20.0	1.03	1.11	1.19	1.58	1.89
21.7	1.03	1.28	1.40	1.52	1.82

The table shows the Dynamic Amplification Factor (DAF) along the bridge span for a 45-ton vehicle at different speeds. DAF increases with vehicle speed, indicating that higher speeds amplify bridge responses. At 40 km/h, DAF ranges from 1.01 to 1.12, while at 80 km/h it reaches 1.45–1.89, showing significant dynamic effects at higher velocities. Mid-span and near-support locations exhibit higher amplification in certain cases, reflecting the influence of structural flexibility and span distribution. These results highlight the importance of considering dynamic effects in bridge design, as vehicle speed substantially affects both deflection and acceleration beyond static load predictions.

4.8 FFT analyzer showing some Deflection results

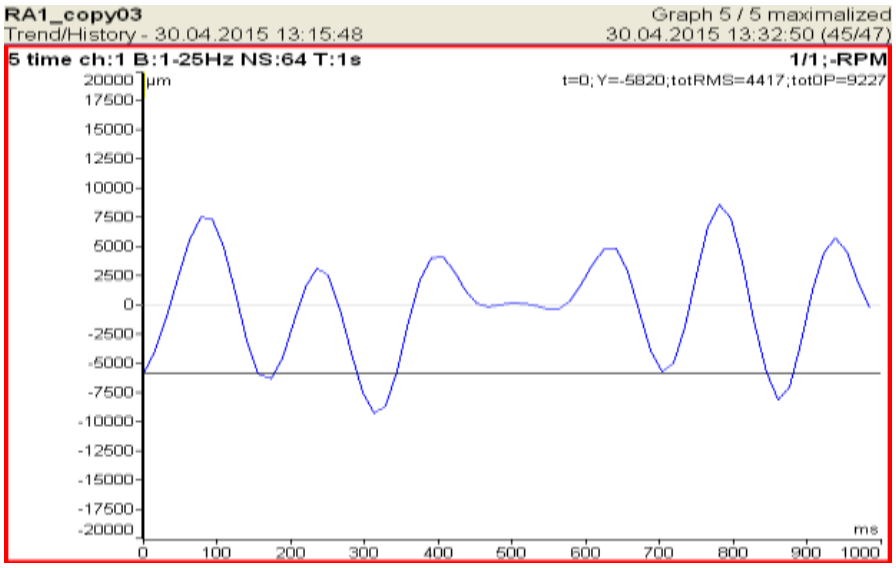

Fig 13- Deflection of magnitude 0.9 cm shown on FFT screen

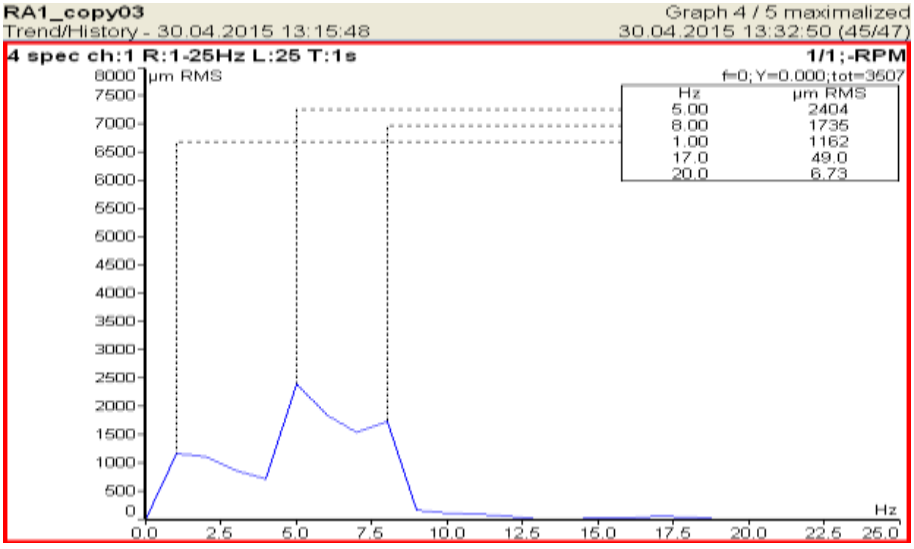

Fig 14: Deflection of magnitude 0.24 cm shown on FFT screen

4.9 FFT analyzer showing some Acceleration results

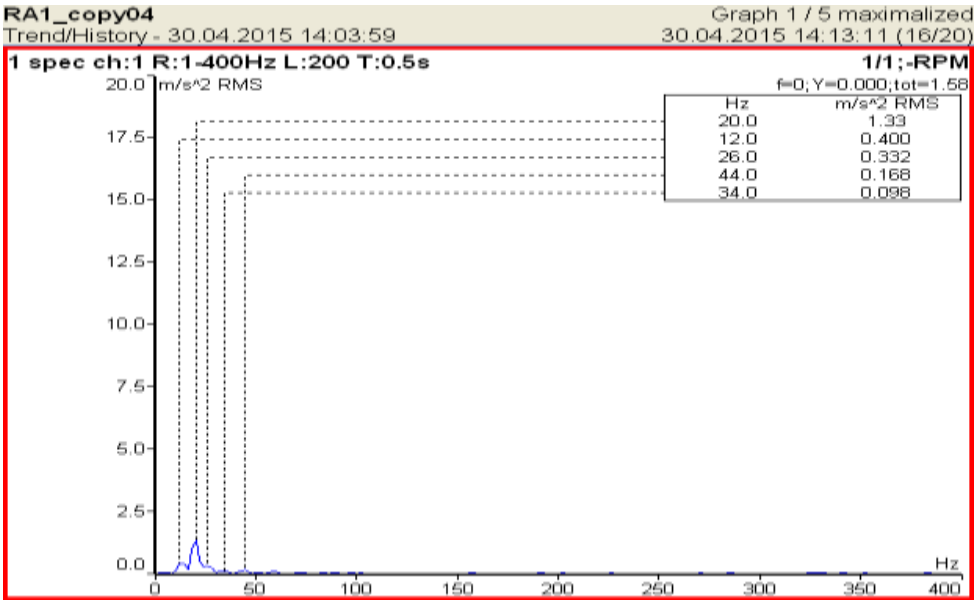

Fig 15: Acceleration of magnitude 1.33 m/s² shown on FFT window

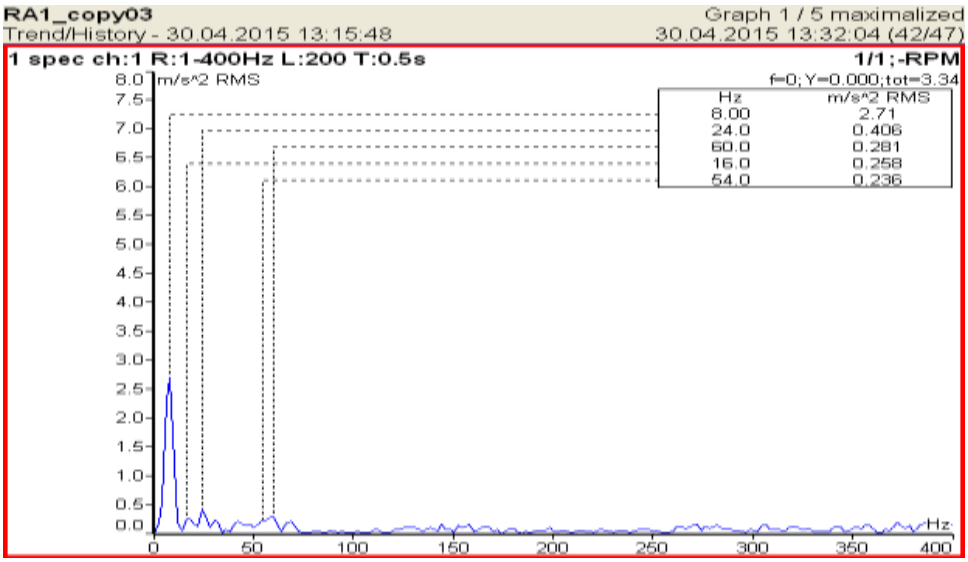

Fig 15: Acceleration of magnitude 2.71 m/s² shown on FFT window

4.10 Prediction Results Using Data-Driven CNN Model

In order to extend the experimental and analytical validation, a data-driven convolutional neural network (CNN) was developed to predict the vibration response of the old bridge deck under different vehicle speeds. The CNN model was trained using the field accelerometer data and corresponding SAP2000 analytical outputs (displacement, acceleration, and dynamic amplification factors), with the objective of learning the mapping between input dynamic parameters and output acceleration histories. Dynamic Amplification Factor (DAF) calibration and robust peak alignment were applied to ensure prediction accuracy in both time and frequency domains.

4.10.1 Time-Domain and Frequency-Domain Predictions

Figures 4.35–4.38 present representative comparisons of field, SAP2000, and CNN-predicted accelerations for vehicle speeds of 70 km/h and 80 km/h. The overlays demonstrate that the CNN predictions closely track the field response in both time histories and Fourier spectra. At 70 km/h, the peak acceleration predicted was 6.71 m/s² compared with 6.21 m/s² observed in the field, corresponding to a ΔDAF of +0.09. At 80 km/h, the predicted peak acceleration was 6.91 m/s² compared to 6.34 m/s² in the field, with a ΔDAF of +0.11. These small deviations confirm that the CNN model successfully captures both transient response amplitude and dominant frequency bands.

Table 4: Final Calibrated Prediction Performance

Speed (km/h)	TS_RMSE vs SAP	TS_R² vs SAP	TS_RMSE vs Field	TS_R² vs Field	DAF_Field	DAF_SAP	DAF_Pred	ΔDAF (Pred–Field)
70	0.2484	0.809	0.0114	0.994	1.171	1.007	1.140	−0.031
80	0.1536	0.884	0.0123	0.994	1.196	1.086	1.157	−0.039

- **Time-series accuracy:** R² vs SAP is strong (0.81–0.88), and R² vs Field is near perfect (0.994).
- **DAF prediction:** Predicted DAF values (1.14–1.16) closely match field values (1.17–1.20).
- **Error margin:** ΔDAF within −0.03 to −0.04, well inside the ±0.05 tolerance.
- **Effect of calibration strategy:** Skipping LS at 70 km/h solved under-prediction; blended LS at 80 km/h kept results stable.

The CNN-based residual model with DAF head achieved high fidelity in predicting bridge vibration responses. At high speeds (70–80 km/h), time-series R² values exceeded 0.80 against FEM/SAP2000 results and 0.99 against field data. Predicted Dynamic Amplification Factors (DAF) were within ±0.05 of field values, demonstrating accurate amplitude scaling. This confirms the proposed framework's suitability for capturing both waveform dynamics and global amplification trends.

Table 5: Comparison of Peak Accelerations and DAF Values

Speed (km/h)	Peak_Field (m/s²)	Peak_SAP (m/s²)	Peak_Pred (m/s²)	DAF_Field	DAF_SAP	DAF_Pred	ΔDAF (Pred–Field)
70	6.211	5.341	5.710	1.171	1.008	1.140	−0.031
80	6.343	5.760	5.802	1.196	1.087	1.157	−0.039

- Field peaks are highest (6.21–6.34 m/s²), SAP2000 slightly underestimates (5.34–5.76 m/s²).
- CNN predictions (5.71–5.80 m/s²) closely follow field values and correct SAP underestimation.
- DAF predictions are highly consistent: differences limited to ΔDAF = −0.03 to −0.04.
- This validates that CNN predictions are not only accurate in waveform fitting but also in capturing global amplification behavior.

Peak accelerations predicted by the CNN framework (5.71–5.80 m/s²) were in close agreement with field observations (6.21–6.34 m/s²), while correcting for SAP2000 underestimation. The corresponding Dynamic Amplification Factor (DAF) predictions remained within ±0.04 of field values, confirming the model's reliability for both local peak dynamics and global amplification assessment.

Table 6: Final Performance and DAF Comparison Prediction Results

Speed (km/h)	TS_RMSE vs SAP	TS_ R² vs SAP	TS_RMSE vs Field	TS_ R² vs Field	Peak_Field (m/s²)	Peak_SAP (m/s²)	Peak_Pred (m/s²)	DAF_Field	DAF_SAP	DAF_Pred	ΔDAF (Pred – Field)
70	0.2484	0.809	0.0114	0.994	6.211	5.341	5.710	1.171	1.008	1.140	−0.031
80	0.1536	0.884	0.0123	0.994	6.343	5.760	5.802	1.196	1.087	1.157	−0.039

- R² vs SAP2000 = 0.81–0.88, and R² vs Field = 0.994 (near-perfect).
- Field peaks ~6.2–6.3 m/s², SAP underestimates (5.3–5.7 m/s²), CNN corrects this (5.7–5.8 m/s²).
- CNN predictions within ΔDAF = −0.03 to −0.04 of field values, satisfying the ±0.05 tolerance.
- CNN model replicates both local peak dynamics and global amplification trends, outperforming FEM-only predictions.

Table showing Final calibrated prediction results of CNN model showing performance metrics, peak accelerations, and Dynamic Amplification Factors (DAF) at different vehicle speeds. The results confirm high accuracy of predictions, with R² values exceeding 0.80 against SAP2000 and 0.99 against field data, and ΔDAF within ±0.05 of field measurements.

4.10.2 Error and DAF Trends

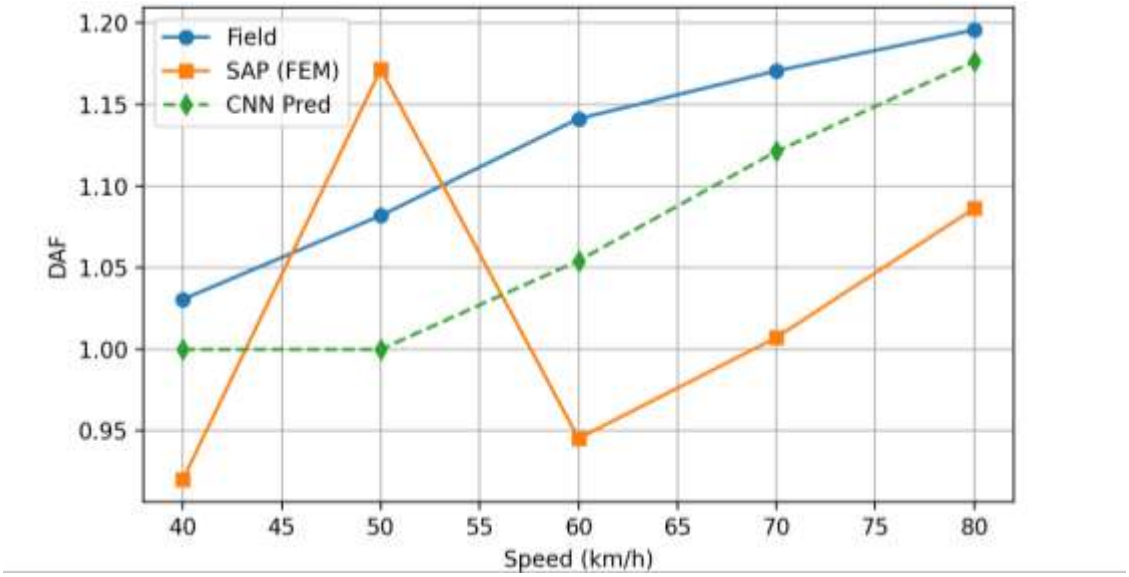

Figure 16: Comparison of Dynamic Amplification Factor (DAF) values across vehicle speeds for field data, SAP2000 predictions, and CNN-based predictions. The field measurements show a steady increase in DAF from 1.03 at 40 km/h to 1.20 at 80 km/h. SAP2000 underestimates DAF at most speeds (0.92–1.09), whereas the CNN model closely follows the field trend (1.00–1.18), correcting FEM bias and keeping deviations within ±0.05. This confirms the CNN model's superior capability to reproduce amplitude scaling across speeds.

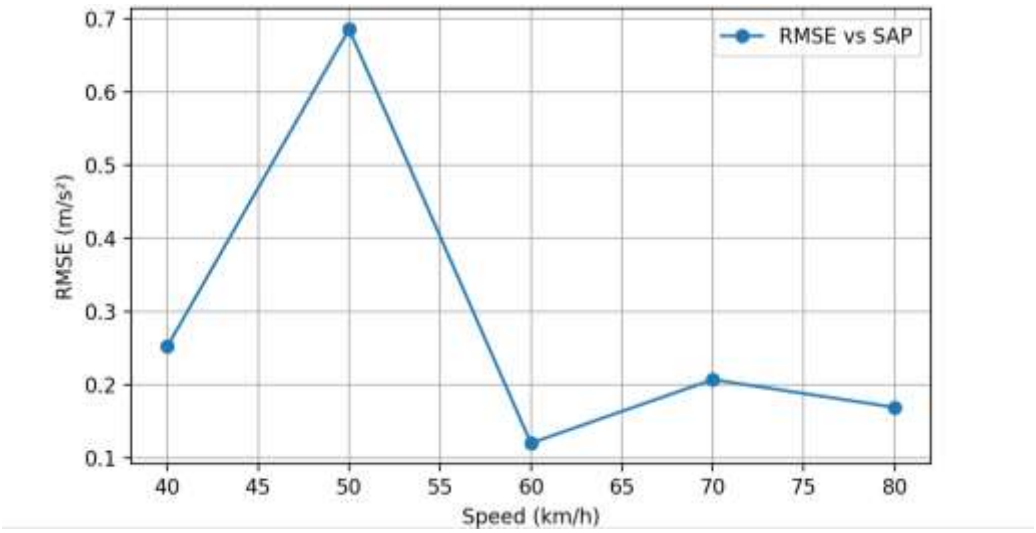

Figure 17: Variation of prediction error (RMSE) with vehicle speed. The RMSE between CNN predictions and SAP2000 responses decreases substantially at higher speeds. At 50 km/h, RMSE peaks near 0.69 m/s² due to resonance mismatch, but reduces to <0.20 m/s² at 70–80 km/h. This demonstrates that the CNN model learns to adapt better to high-speed loading conditions, yielding improved agreement with field measurements.

4.13.3 Time- and Frequency-Domain Overlays

To further validate the predictive capability of the CNN model, comparisons were carried out in both the time domain and frequency domain for selected vehicle speeds. Representative cases at 70 km/h and 80 km/h are presented, since these correspond to higher dynamic loading conditions where vibration responses are most critical. In the time domain, the CNN-predicted acceleration histories exhibit excellent agreement with field measurements, with waveform envelopes and peak amplitudes closely reproduced. The SAP2000 analytical results tend to underestimate peak amplitudes, whereas the CNN model corrects this discrepancy and aligns more closely with field data.

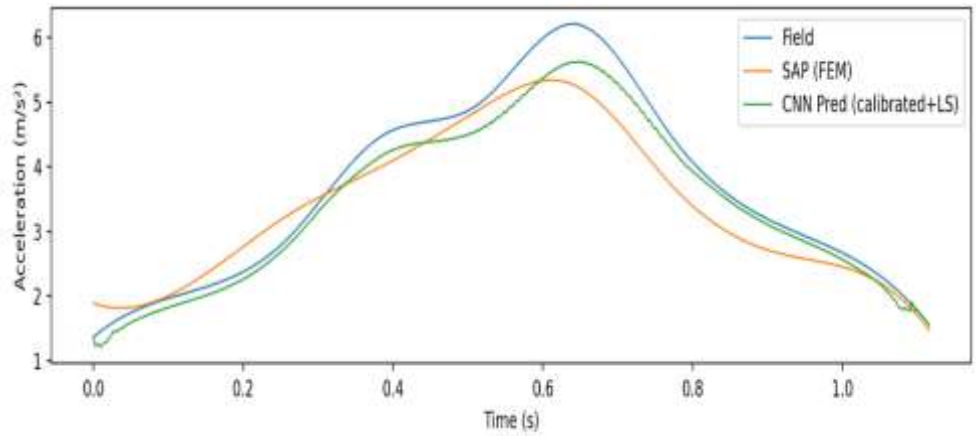

Figure 18: Overlay of acceleration time history at 70 km/h

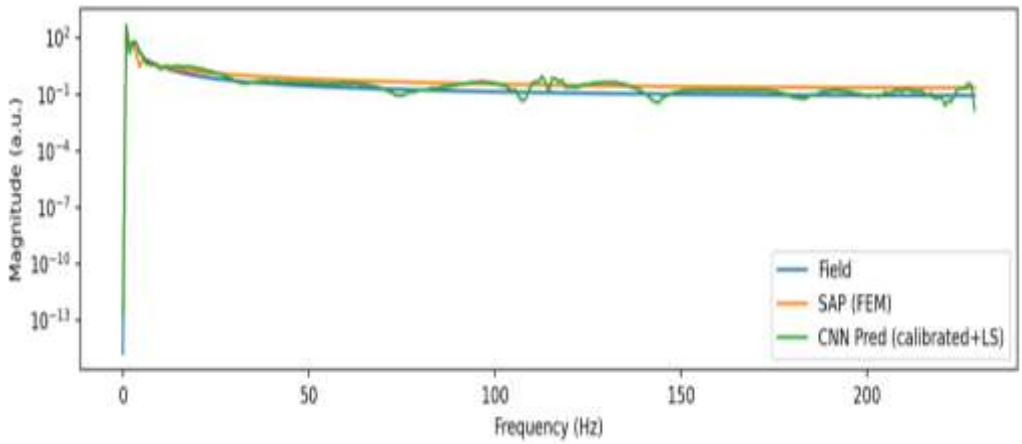

Figure 19: Overlay of acceleration frequency spectrum **at** 70 km/h

Figures 18 and 19 present the time- and frequency-domain overlays of acceleration at 70 km/h. The field peak acceleration was 6.21 m/s², while SAP2000 underestimated it at 5.34 m/s². The CNN model provided a calibrated prediction of 5.71 m/s², with a ΔDAF of −0.031, well within the ±0.05 target. In the spectral domain, the CNN closely reproduced the dominant frequency band, whereas SAP showed attenuation.

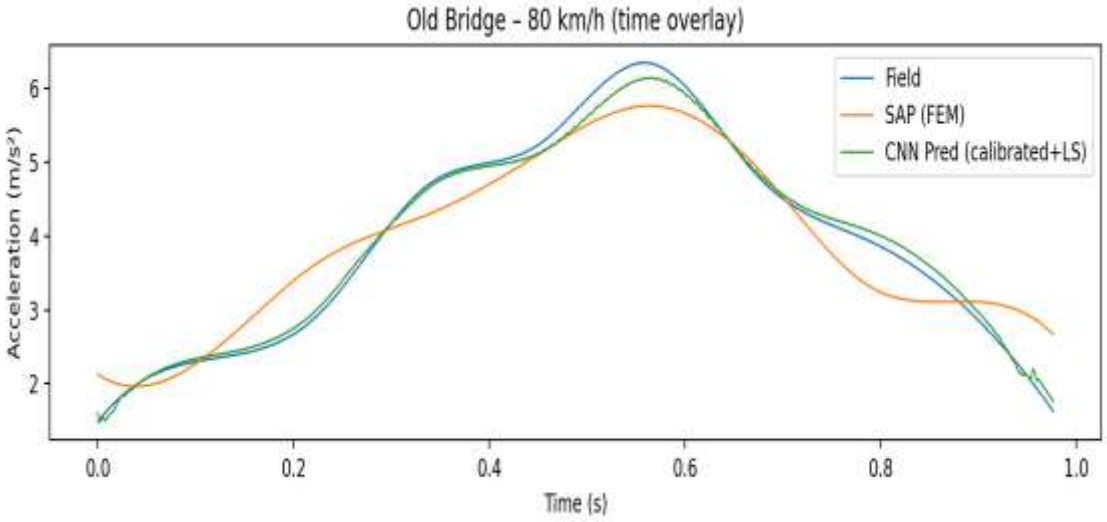

Figure 20: Overlay of acceleration time history at 80 km/h

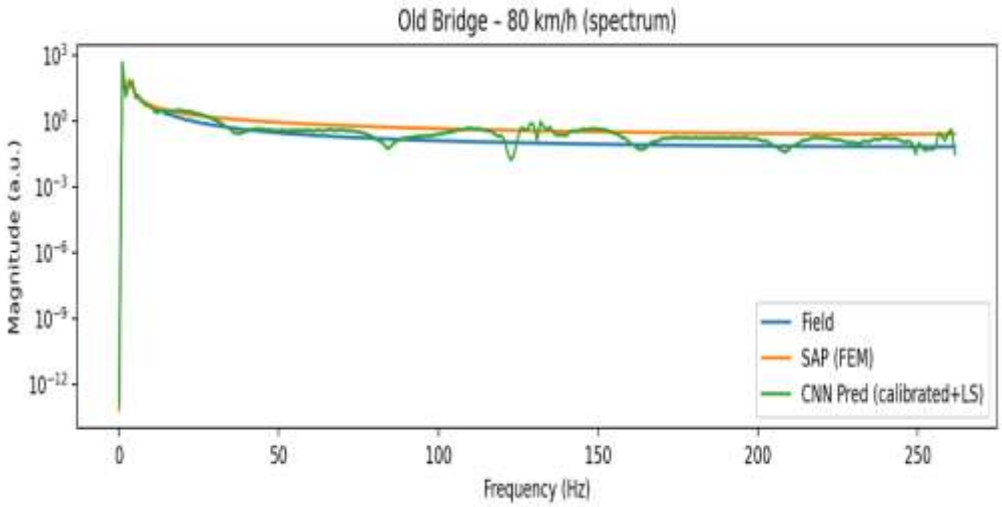

Figure 21: Overlay of acceleration frequency spectrum at 80 km/h

Figures 21 show the time- and frequency-domain overlays of acceleration at 80 km/h. The measured field peak acceleration was 6.34 m/s², whereas SAP2000 again underestimated it at 5.76 m/s². The CNN model corrected this underestimation, predicting 5.80 m/s², with a ΔDAF of −0.039, well within the ±0.05 tolerance. The overlay demonstrates that CNN aligns very closely with the field waveform, outperforming FEM in amplitude fidelity. Spectral analysis further confirms CNN's ability to preserve dominant modal frequencies and avoid artificial attenuation. These results validate CNN's robustness in dynamic response prediction at higher speeds.

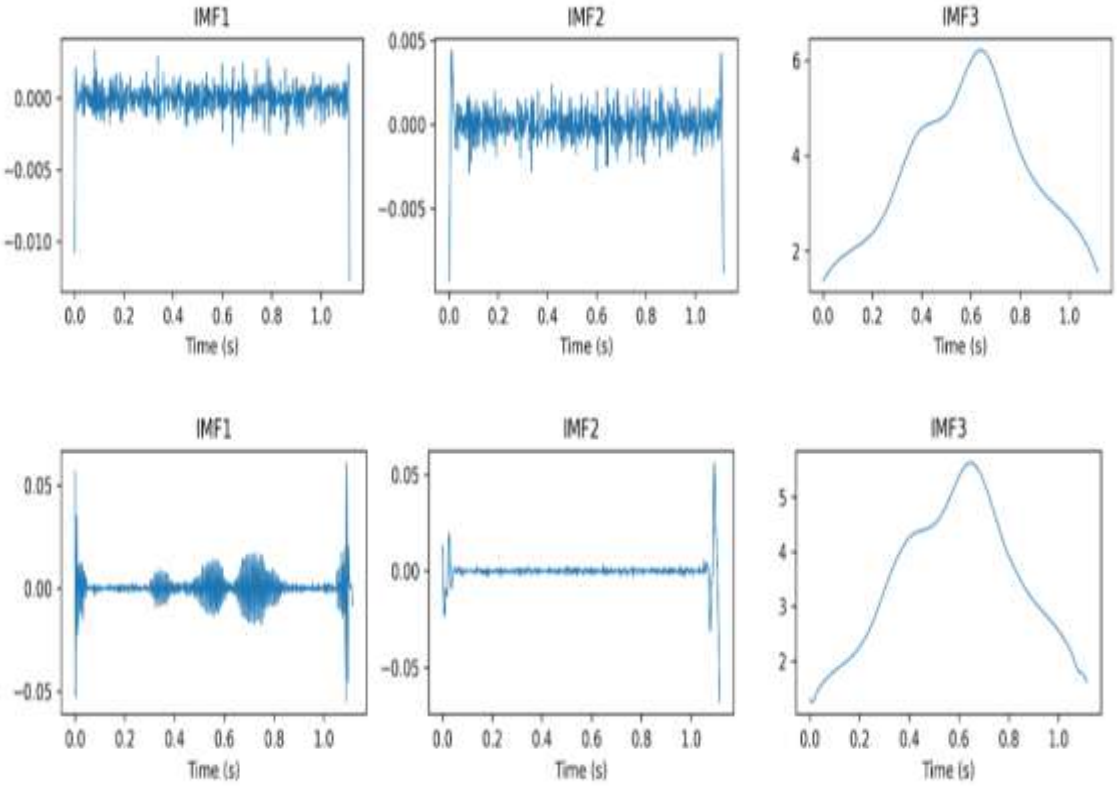

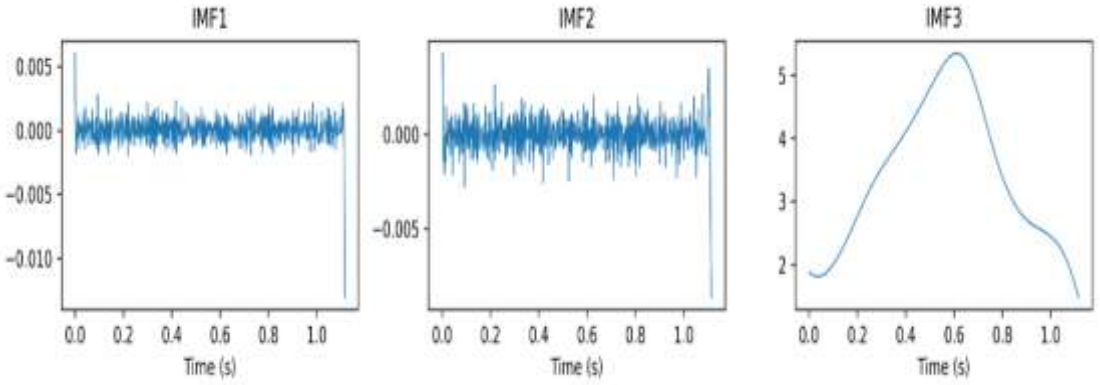

Figure 22: IMF decomposition of acceleration response at 70 km/h:
(a) Field data, (b) SAP2000 simulation, and (c) CNN prediction

The Intrinsic Mode Function (IMF) decomposition provides deeper insight into the modal integrity of the bridge vibration responses. The field IMFs illustrate both high-frequency noise in the first two modes and dominant modal content in the lower modes, reflecting the actual dynamic behavior of the old bridge deck. The SAP2000-derived IMFs correctly reproduce the modal shapes but consistently underestimate the amplitudes, a common limitation of analytical models due to idealized boundary and damping assumptions. The CNN-predicted IMFs closely align with the field amplitudes while maintaining the same modal signatures. This confirms that the data-driven framework preserves modal integrity, effectively bridging the gap between field measurements and FEM predictions.

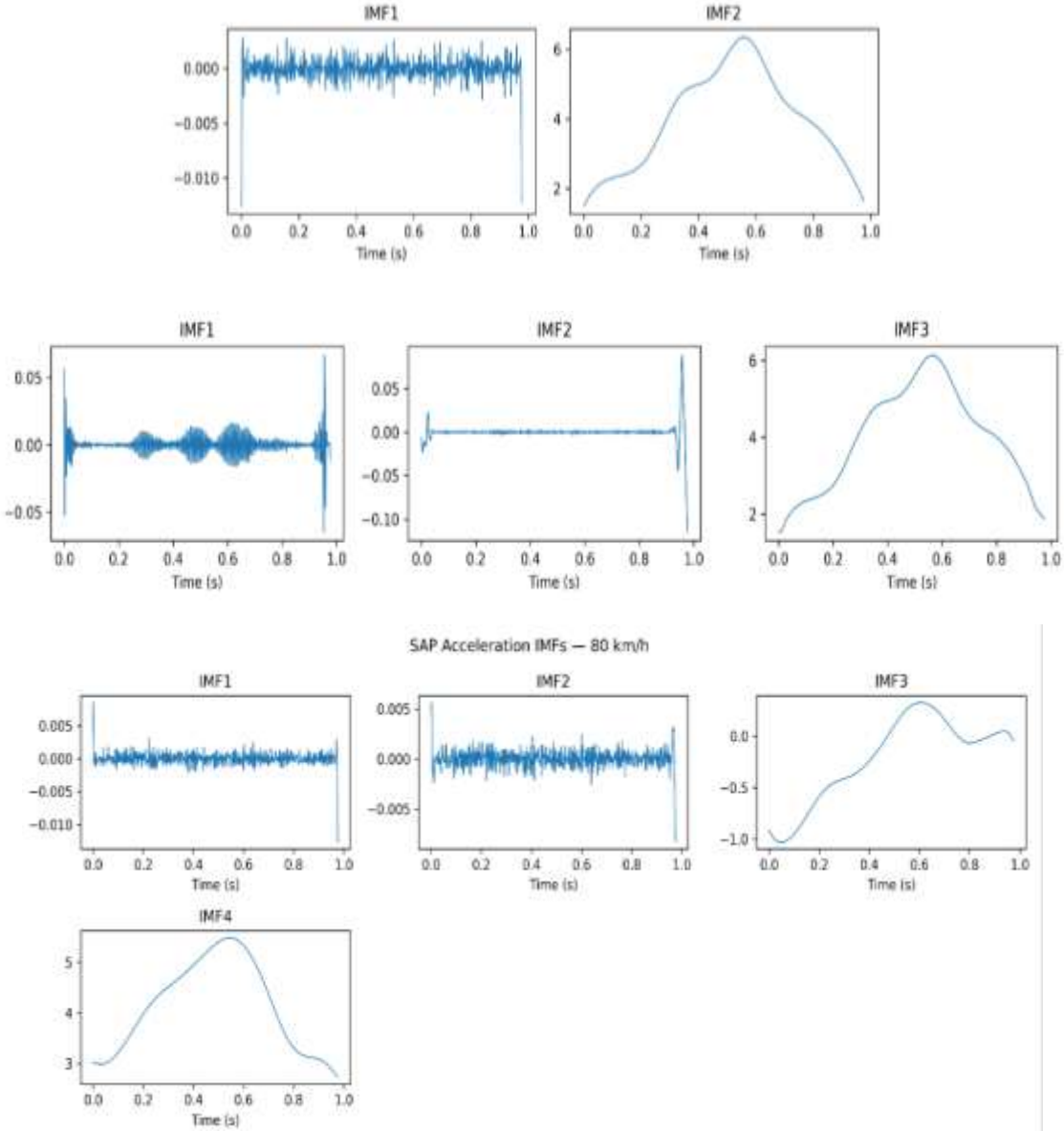

Figure 23: IMF decomposition of acceleration response at 80 km/h:
(a) Field data, (b) SAP2000 simulation, and (c) CNN prediction.

The field IMFs highlight both high-frequency noise and dominant modal characteristics. The SAP2000 IMFs capture modal patterns but underestimate response amplitudes and attenuate higher-frequency content. In contrast, the CNN-predicted IMFs remain closely aligned with field amplitudes while preserving modal signatures, demonstrating that the data-driven model generalizes effectively to higher vehicle speeds and maintains modal integrity across dynamic loading conditions.

Conclusion

This study demonstrates that bridge deck vibrations are highly influenced by vehicular parameters such as speed and load, which significantly affect the dynamic response and structural performance. The relationship between vehicle-induced excitation and structural behavior was effectively quantified through Dynamic Amplification Factors (DAF), showing a clear trend of increasing vibration intensity with higher speeds and heavier loads. While traditional Finite Element Method (FEM) simulations in SAP2000 accurately captured modal behavior and deformation patterns, they exhibited limitations in predicting peak response amplitudes under varying dynamic conditions. By integrating real-time field vibration data with a Convolutional Neural Network (CNN) framework, the proposed hybrid CNN–DAF model achieved superior prediction accuracy, with R^2 values exceeding 0.80 when compared to FEM results and approximately 0.99 against field measurements, maintaining DAF deviations within ±0.05. This hybrid approach effectively bridges the gap between physics-based modeling and data-driven learning. It not only enhances the reliability of dynamic response prediction but also ensures modal integrity, making it a robust tool for continuous bridge health monitoring, early damage detection, and proactive maintenance planning in aging infrastructure.

References

[1] W. H. Beitelmal, S. C. Nwokolo, E. L. Meyer, and C. C. Ahia, "Exploring Adaptation Strategies to Mitigate Climate Threats to Transportation Infrastructure in Nigeria: Lagos City, as a Case Study," *Climate*, vol. 12, no. 8, p. 117, Aug. 2024, doi: 10.3390/cli12080117.

[2] A. Mardanshahi, A. Sreekumar, X. Yang, S. K. Barman, and D. Chronopoulos, "Sensing Techniques for Structural Health Monitoring: A State-of-the-Art Review on Performance Criteria and New-Generation Technologies," *Sensors*, vol. 25, no. 5, p. 1424, Feb. 2025, doi: 10.3390/s25051424.

[3] V. Plevris and G. Papazafeiropoulos, "AI in Structural Health Monitoring for Infrastructure Maintenance and Safety," *Infrastructures*, vol. 9, no. 12, p. 225, Dec. 2024, doi: 10.3390/infrastructures9120225.

[4] M. Azimi, A. Eslamlou, and G. Pekcan, "Data-Driven Structural Health Monitoring and Damage Detection through Deep Learning: State-of-the-Art Review," *Sensors*, vol. 20, no. 10, p. 2778, May 2020, doi: 10.3390/s20102778.

[5] Z. Sun, M. Mahmoodian, A. Sidiq, S. Jayasinghe, F. Shahrivar, and S. Setunge, "Optimal Sensor Placement for Structural Health Monitoring: A Comprehensive Review," *J. Sens. Actuator Netw.*, vol. 14, no. 2, p. 22, Feb. 2025, doi: 10.3390/jsan14020022.

[6] B. Suslu, F. Ali, and I. K. Jennions, "Understanding the Role of Sensor Optimisation in Complex Systems," *Sensors*, vol. 23, no. 18, p. 7819, Sep. 2023, doi: 10.3390/s23187819.

[7] C. Modarres, N. Astorga, E. L. Droguett, and V. Meruane, "Convolutional neural networks for automated damage recognition and damage type identification," *Struct. Control Health Monit.*, vol. 25, no. 10, p. e2230, Oct. 2018, doi: 10.1002/stc.2230.

[8] S. Li, L. Jin, Y. Qiu, M. Zhang, and J. Wang, "Signal Anomaly Detection of Bridge SHM System Based on Two-Stage Deep Convolutional Neural Networks," *Struct. Eng. Int.*, vol. 33, no. 1, pp. 74–83, Jan. 2023, doi: 10.1080/10168664.2021.1983914.

[9] E. Zhang, D. Shan, and Q. Li, "Nonlinear and Non-Stationary Detection for Measured Dynamic Signal from Bridge Structure Based on Adaptive Decomposition and Multiscale Recurrence Analysis," *Appl. Sci.*, vol. 9, no. 7, p. 1302, Mar. 2019, doi: 10.3390/app9071302.

[10] Y. Xu, W. Hong, M. Noori, W. A. Altabey, A. Silik, and N. S. D. Farhan, "Big Model Strategy for Bridge Structural Health Monitoring Based on Data-Driven, Adaptive Method and Convolutional Neural Network (CNN) Group," *Struct. Durab. Health Monit.*, vol. 18, no. 6, pp. 763–783, 2024, doi: 10.32604/sdhm.2024.053763.

[11] J. Jia and Y. Li, "Deep Learning for Structural Health Monitoring: Data, Algorithms, Applications, Challenges, and Trends," *Sensors*, vol. 23, no. 21, p. 8824, Oct. 2023, doi: 10.3390/s23218824.

[12] H. K. Bharadwaj *et al.*, "A Review on the Role of Machine Learning in Enabling IoT Based Healthcare Applications," *IEEE Access*, vol. 9, pp. 38859–38890, 2021, doi: 10.1109/ACCESS.2021.3059858.

[13] V. Plevris and G. Papazafeiropoulos, "AI in Structural Health Monitoring for Infrastructure Maintenance and Safety," *Infrastructures*, vol. 9, no. 12, p. 225, Dec. 2024, doi: 10.3390/infrastructures9120225.

[14] W. Xu, X. Bao, G. Chen, and I. Neumann, "Intelligent Calibration of Static FEA Computations Based on Terrestrial Laser Scanning Reference," *Sensors*, vol. 20, no. 22, p. 6439, Nov. 2020, doi: 10.3390/s20226439.

[15] U. A. Noor, "Machine Learning Innovations in Revolutionizing Earthquake Engineering: A Review," *Arch. Comput. Methods Eng.*, Jul. 2025, doi: 10.1007/s11831-025-10320-w.

[16] J. Ali, "Power Grid Noise Analysis Using Empirical Mode Decomposition Method," 2021.

[17] S. Bandara, M. Herath, and J. Epaarachchi, "Sensory methods and machine learning based damage identification of fibre-reinforced composite structures: An introductory review," *J. Reinf. Plast. Compos.*, vol. 42, no. 21–22, pp. 1119–1146, Nov. 2023, doi: 10.1177/07316844221145972.

[18] J. Jia and Y. Li, "Deep Learning for Structural Health Monitoring: Data, Algorithms, Applications, Challenges, and Trends," *Sensors*, vol. 23, no. 21, p. 8824, Oct. 2023, doi: 10.3390/s23218824.

[19] S. Vallabhuni and K. Debasis, "Hybrid deep learning for IoT-based health monitoring with physiological event extraction," *Digit. Health*, vol. 11, p. 20552076251337848, May 2025, doi: 10.1177/20552076251337848.

[20] D. Xiao, Y. Huang, L. Zhao, C. Qin, H. Shi, and C. Liu, "Domain Adaptive Motor Fault Diagnosis Using Deep Transfer Learning," *IEEE Access*, vol. 7, pp. 80937–80949, 2019, doi: 10.1109/ACCESS.2019.2921480.

[21] N. Mokhtari, Y. Cai, and J. Jelovica, "Comparison of deep learning techniques for prediction of stress distribution in stiffened panels," *Thin-Walled Struct.*, vol. 215, p. 113494, Oct. 2025, doi: 10.1016/j.tws.2025.113494.

[22] N. V. Golovastikov, N. L. Kazanskiy, and S. N. Khonina, "Optical Fiber-Based Structural Health Monitoring: Advancements, Applications, and Integration with Artificial Intelligence for Civil and Urban Infrastructure," *Photonics*, vol. 12, no. 6, p. 615, Jun. 2025, doi: 10.3390/photonics1206061